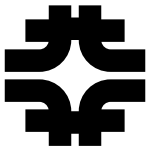

Fermi National Accelerator Laboratory

FERMILAB-Pub-96/023-A

Loop Corrections in Non-Linear Cosmological Perturbation Theory II. Two-point Statistics and Self-Similarity

R. Scoccimarro and J.A. Frieman

Fermi National Accelerator Laboratory
P.O. Box 500, Batavia, Illinois 60510

February 1996

Operated by Universities Research Association Inc. under Contract No. DE-AC02-76CHO3000 with the United States Department of Energy

Disclaimer

FERMILAB-Pub-96/023-A

Loop Corrections in Non-Linear Cosmological Perturbation Theory II. Two-point Statistics and Self-Similarity

Román Scoccimarro[1,2] and Joshua A. Frieman[2,3]

[1]Department of Physics and Enrico Fermi Institute, University of Chicago, Chicago, IL 60637

[2]NASA/Fermilab Astrophysics Center, Fermi National Accelerator Laboratory, P.O.Box 500, Batavia, IL 60510

ABSTRACT

We calculate the lowest-order non-linear contributions to the power spectrum, two-point correlation function, and smoothed variance of the density field, for Gaussian initial conditions and scale-free initial power spectra, $P(k) \sim k^n$. These results extend and in some cases correct previous work in the literature on cosmological perturbation theory. Comparing with the scaling behavior observed in N-body simulations, we find that the validity of non-linear perturbation theory depends strongly on the spectral index n. For $n < -1$, we find excellent agreement over scales where the variance $\sigma^2(R) \lesssim 10$; however, for $n \geq -1$, perturbation theory predicts deviations from self-similar scaling (which increase with n) not seen in numerical simulations. This anomalous scaling suggests that the principal assumption underlying cosmological perturbation theory, that large-scale fields can be described perturbatively even when fluctuations are highly non-linear on small scales, breaks down beyond leading order for spectral indices $n \geq -1$. For $n < -1$, the power spectrum, variance, and correlation function in the scaling regime can be calculated using dimensional regularization.

Subject headings: cosmology: large-scale structure of the universe

---

[3]Also Department of Astronomy and Astrophysics, University of Chicago, Chicago, IL 60637

1. Introduction

Several independent arguments suggest that the growth of cosmological density perturbations on large scales can be described by perturbation theory, even when the density and velocity fields are highly non-linear on small scales. For example, analytic and numerical work showed that linear perturbation theory describes the evolution of the large-scale density power spectrum $P(k)$, provided the initial spectrum falls off less steeply than k^4 for small k (Zel'dovich 1965, Peebles 1974, Peebles & Groth 1976, Peebles 1980). In addition, for Gaussian initial conditions, leading-order non-linear perturbative calculations of higher order moments of the density field, e.g., the skewness and kurtosis, agree well with N-body simulations in the weakly non-linear regime, where the variance of the smoothed density field $\sigma^2(R) \equiv \langle \delta^2(R) \rangle \lesssim 0.5 - 1$ (Juszkiewicz, Bouchet & Colombi 1993, Bernardeau 1994, Gaztañaga & Baugh 1995, Baugh, Gaztañaga & Efstathiou 1995). Thus, leading-order perturbation theory has been shown to work surprisingly well in the cases where comparisons with numerical simulations have been made.

The success of leading-order cosmological perturbation theory raises questions: since the perturbation series is most likely asymptotic, what happens beyond leading order—does the agreement with simulations improve or deteriorate? More generally, what sets the limits of perturbation theory, beyond which it breaks down? These questions have become more urgent since it has been shown that leading-order perturbation theory appears to provide an adequate description even on scales where *next-to-leading order* and higher order perturbative contributions would be expected to become important.

To address these questions, one must calculate loop corrections, *i.e.*, corrections *beyond* leading order, in non-linear cosmological perturbation theory (NLCPT). This is the second paper of a series devoted to this topic. In the first paper (Scoccimarro & Frieman 1996), we applied diagrammatic techniques to calculate loop corrections to 1-point cumulants of unsmoothed fields, such as the variance and skewness, for Gaussian initial conditions. Here, we calculate the 1-loop (first non-linear) corrections to the power spectrum, the volume-averaged two-point correlation function, and the variance of the smoothed density field for scale-free initial spectra, $P(k) \sim k^n$. While the linear power spectrum for the Universe is not scale-free (on both observational and theoretical grounds), scale-free spectra are useful approximations over limited ranges of wavenumber k; they also have the advantage of yielding analytic closed form results. In a forthcoming paper, we will present 1-loop corrections to the bispectrum (the three-point cumulant in Fourier space) and the skewness of the smoothed density field for scale-free and cold dark matter spectra.

One-loop corrections to the two-point correlation function and power spectrum have been previously studied in the literature (Juszkiewicz 1981, Vishniac 1983, Juszkiewicz,

Sonoda & Barrow 1984, Coles 1990, Suto & Sasaki 1991, Makino, Sasaki & Suto 1992, Jain & Bertschinger 1994, Baugh & Efstathiou 1994). Multi-loop corrections to the power spectrum were considered by Fry 1994, including the full contributions up to 2 loops and the most important terms at large k in 3- and 4-loop order. Some of our results overlap in particular with the analytic results for the 1-loop power spectrum reported by Suto & Sasaki (1991) and in Makino et al. (1992). However, since we found that some of their expressions contain errors, we present complete corrected expressions for the 1-loop power spectrum. One-loop corrections to the variance were studied numerically for Gaussian smoothing by Lokas et al. (1995). We correct some numerical errors in their results, extend them to include top-hat smoothing and to the average two-point correlation function, and provide analytic derivation of some of the numerical results.

The limiting behavior of the 1-loop corrections on large scales leads us to reconsider the issue of self-similarity in perturbation theory (Davis & Peebles 1977, Peebles 1980). It is commonly accepted that the evolution of density perturbations from scale-free initial conditions in an Einstein-de Sitter universe is statistically self-similar. N-body simulations have generally found self-similar scaling for $-3 < n < 1$, although the results for $n < -1$ have been somewhat ambiguous due to problems of dynamic range in the simulations (Efstathiou et al. 1988, Bertschinger & Gelb 1991, Ryden & Gramann 1991, Gramann 1992, Colombi et al. 1995, Jain 1995, Padmanabhan et al. 1995). The issue of self-similarity in NLCPT has recently been investigated by Jain & Bertschinger (1995), who present arguments that the perturbative evolution is also self-similar. While we do not disagree with their calculations, we start from a different premise regarding cutoffs in the initial spectrum, which leads us to conclude that loop corrections break self-similar scaling if the spectral index $n \geq -1$. In the regime where we do find scaling, $n < -1$, we use dimensional regularization to calculate analytically the asymptotic behavior of the 1-loop power spectrum, variance, and average correlation function; these results agree quite well with the 'universal scaling' extracted from numerical simulations (Hamilton et al. 1991, Peacock & Dodds 1994, Jain, Mo & White 1995).

The paper is organized as follows. In Sec. 2 we discuss non-linear perturbation theory and review the diagrammatic approach developed in (Fry 1984, Goroff et al. 1986, Scoccimarro & Frieman 1996) to the calculation of statistical quantities. Section 3 presents the results of 1-loop calculations for the power spectrum, the smoothed variance, and average two-point correlation function. Self-similarity in perturbation theory is the subject of Sec. 4. We discuss the conditions under which 1-loop corrections exhibit self-similarity and compare our results with the universal scaling hypothesis, based on numerical simulations. Section 5 contains our conclusions.

2. Dynamics and Statistics

2.1. The Equations of Motion

Assuming the universe is dominated by pressureless dust (e.g., cold dark matter), in the single-stream approximation (prior to orbit crossing) one can adopt a fluid description of the cosmological N-body problem. In this limit, the relevant equations of motion correspond to conservation of mass and momentum and the Poisson equation (e.g., Peebles 1980, Scoccimarro & Frieman 1996),

$$\frac{\partial \delta(\mathbf{x},\tau)}{\partial \tau} + \nabla \cdot \{[1+\delta(\mathbf{x},\tau)]\mathbf{v}(\mathbf{x},\tau)\} = 0, \tag{2-1a}$$

$$\frac{\partial \mathbf{v}(\mathbf{x},\tau)}{\partial \tau} + \mathcal{H}(\tau)\ \mathbf{v}(\mathbf{x},\tau) + [\mathbf{v}(\mathbf{x},\tau)\cdot\nabla]\mathbf{v}(\mathbf{x},\tau) = -\nabla\Phi(\mathbf{x},\tau), \tag{2-1b}$$

$$\nabla^2\Phi(\mathbf{x},\tau) = \frac{3}{2}\Omega\mathcal{H}^2(\tau)\delta(\mathbf{x},\tau) \tag{2-1c}$$

Here the density contrast $\delta(\mathbf{x},\tau) \equiv \rho(\mathbf{x},\tau)/\bar{\rho} - 1$, with $\bar{\rho}(\tau)$ the mean density of matter, $\mathbf{v} \equiv d\mathbf{x}/d\tau$ represents the velocity field fluctuations about the Hubble flow, $\mathcal{H} \equiv d\ln a/d\tau$ is the conformal expansion rate, $a(\tau)$ is the cosmic scale factor, $\mathbf{x}$ denote comoving coordinates, $\tau = \int dt/a$ is the conformal time, Φ is the gravitational potential due to the density fluctuations, and the density parameter $\Omega = \bar{\rho}/\rho_c = 8\pi G\bar{\rho}a^2/3\mathcal{H}^2$. Note that we have implicitly assumed the Newtonian approximation to General Relativity, valid on scales less than the Hubble length $a\mathcal{H}^{-1}$. We take the velocity field to be irrotational, so it can be completely described by its divergence $\theta \equiv \nabla\cdot\mathbf{v}$. Equations (2-1) hold in an arbitrary homogeneous and isotropic background Universe which evolves according to the Friedmann equations; henceforth, for simplicity we assume an Einstein-de Sitter background, $\Omega = 1$ (with vanishing cosmological constant), for which $a \propto \tau^2$ and $3\Omega\mathcal{H}^2/2 = 6/\tau^2$.

We take the divergence of Equation (2-1b) and Fourier transform the resulting equations of motion according to the convention

$$\tilde{A}(\mathbf{k},\tau) = \int \frac{d^3x}{(2\pi)^3}\exp(-i\mathbf{k}\cdot\mathbf{x})\ A(\mathbf{x},\tau), \tag{2-2}$$

for the Fourier transform of any field $A(\mathbf{x},\tau)$, where, here and throughout, $\mathbf{k}$ is a comoving wavenumber. This yields

$$\frac{\partial\tilde{\delta}(\mathbf{k},\tau)}{\partial\tau} + \tilde{\theta}(\mathbf{k},\tau) = -\int d^3k_1 \int d^3k_2 \delta_D(\mathbf{k}-\mathbf{k}_1-\mathbf{k}_2)\alpha(\mathbf{k},\mathbf{k}_1)\tilde{\theta}(\mathbf{k}_1,\tau)\tilde{\delta}(\mathbf{k}_2,\tau), \qquad (2\text{-}3a)$$

$$\begin{aligned}\frac{\partial\tilde{\theta}(\mathbf{k},\tau)}{\partial\tau} &+ \mathcal{H}(\tau)\,\tilde{\theta}(\mathbf{k},\tau) + \frac{3}{2}\mathcal{H}^2(\tau)\tilde{\delta}(\mathbf{k},\tau) = \\ &- \int d^3k_1 \int d^3k_2 \delta_D(\mathbf{k}-\mathbf{k}_1-\mathbf{k}_2)\beta(\mathbf{k},\mathbf{k}_1,\mathbf{k}_2)\tilde{\theta}(\mathbf{k}_1,\tau)\tilde{\theta}(\mathbf{k}_2,\tau), \qquad (2\text{-}3b)\end{aligned}$$

(δ_D denotes the three-dimensional Dirac delta distribution), where the functions

$$\alpha(\mathbf{k},\mathbf{k}_1) \equiv \frac{\mathbf{k}\cdot\mathbf{k}_1}{k_1^2}, \qquad \beta(\mathbf{k},\mathbf{k}_1,\mathbf{k}_2) \equiv \frac{k^2(\mathbf{k}_1\cdot\mathbf{k}_2)}{2k_1^2k_2^2} \qquad (2\text{-}4)$$

encode the non-linearity of the evolution (mode coupling) and come from the non-linear terms in the continuity equation (2-1a) and the Euler equation (2-1b) respectively.

2.2. Perturbation Theory Solutions

Equations (2-3) are very difficult to solve in general, being coupled integro-differential equations with no small parameter. The perturbative approach to the problem is to consider perturbations about the linear solution, effectively treating the variance of the linear fluctuations as a small parameter. In this case, Eqs. (2-3) can be formally solved via a perturbative expansion,

$$\tilde{\delta}(\mathbf{k},\tau) = \sum_{n=1}^{\infty} a^n(\tau)\delta_n(\mathbf{k}), \qquad \tilde{\theta}(\mathbf{k},\tau) = \mathcal{H}(\tau)\sum_{n=1}^{\infty} a^n(\tau)\theta_n(\mathbf{k}), \qquad (2\text{-}5)$$

where only the fastest growing mode is taken into account. At small a, the series are dominated by their first terms, and since $\theta_1(\mathbf{k}) = -\delta_1(\mathbf{k})$ from the continuity equation, $\delta_1(\mathbf{k})$ completely characterizes the linear fluctuations. The equations of motion (2-3) determine $\delta_n(\mathbf{k})$ and $\theta_n(\mathbf{k})$ in terms of the linear fluctuations,

$$\delta_n(\mathbf{k}) = \int d^3q_1 \ldots \int d^3q_n \delta_D(\mathbf{k}-\mathbf{q}_1-\ldots-\mathbf{q}_n)F_n^{(s)}(\mathbf{q}_1,\ldots,\mathbf{q}_n)\delta_1(\mathbf{q}_1)\ldots\delta_1(\mathbf{q}_n), \qquad (2\text{-}6a)$$

$$\theta_n(\mathbf{k}) = -\int d^3q_1 \ldots \int d^3q_n \delta_D(\mathbf{k}-\mathbf{q}_1-\ldots-\mathbf{q}_n)G_n^{(s)}(\mathbf{q}_1,\ldots,\mathbf{q}_n)\delta_1(\mathbf{q}_1)\ldots\delta_1(\mathbf{q}_n), \qquad (2\text{-}6b)$$

where $F_n^{(s)}$ and $G_n^{(s)}$ are symmetric homogeneous functions of the wave vectors $\{\mathbf{q}_1, \ldots, \mathbf{q}_n\}$ with degree zero. They are constructed from the fundamental mode coupling functions $\alpha(\mathbf{k}, \mathbf{k}_1)$ and $\beta(\mathbf{k}, \mathbf{k}_1, \mathbf{k}_2)$ according to the recursion relations ($n \geq 2$, see Goroff et al. (1986), Jain & Bertschinger (1994), for a derivation):

$$\begin{aligned} F_n(\mathbf{q}_1, \ldots, \mathbf{q}_n) &= \sum_{m=1}^{n-1} \frac{G_m(\mathbf{q}_1, \ldots, \mathbf{q}_m)}{(2n+3)(n-1)} \Big[(2n+1)\alpha(\mathbf{k}, \mathbf{k}_1) F_{n-m}(\mathbf{q}_{m+1}, \ldots, \mathbf{q}_n) \\ &+ 2\beta(\mathbf{k}, \mathbf{k}_1, \mathbf{k}_2) G_{n-m}(\mathbf{q}_{m+1}, \ldots, \mathbf{q}_n) \Big], \end{aligned} \tag{2-7a}$$

$$\begin{aligned} G_n(\mathbf{q}_1, \ldots, \mathbf{q}_n) &= \sum_{m=1}^{n-1} \frac{G_m(\mathbf{q}_1, \ldots, \mathbf{q}_m)}{(2n+3)(n-1)} \Big[3\alpha(\mathbf{k}, \mathbf{k}_1) F_{n-m}(\mathbf{q}_{m+1}, \ldots, \mathbf{q}_n) \\ &+ 2n\beta(\mathbf{k}, \mathbf{k}_1, \mathbf{k}_2) G_{n-m}(\mathbf{q}_{m+1}, \ldots, \mathbf{q}_n) \Big], \end{aligned} \tag{2-7b}$$

(where $\mathbf{k}_1 \equiv \mathbf{q}_1 + \ldots + \mathbf{q}_m$, $\mathbf{k}_2 \equiv \mathbf{q}_{m+1} + \ldots + \mathbf{q}_n$, $\mathbf{k} \equiv \mathbf{k}_1 + \mathbf{k}_2$, and $F_1 = G_1 \equiv 1$) and the symmetrization procedure:

$$F_n^{(s)}(\mathbf{q}_1, \ldots, \mathbf{q}_n) = \frac{1}{n!} \sum_{\pi} F_n(\mathbf{q}_{\pi(1)}, \ldots, \mathbf{q}_{\pi(n)}), \tag{2-8a}$$

$$G_n^{(s)}(\mathbf{q}_1, \ldots, \mathbf{q}_n) = \frac{1}{n!} \sum_{\pi} G_n(\mathbf{q}_{\pi(1)}, \ldots, \mathbf{q}_{\pi(n)}), \tag{2-8b}$$

where the sum is taken over all the permutations π of the set $\{1, \ldots, n\}$. For example, for $n = 2$ we have:

$$F_2^{(s)}(\mathbf{q}_1, \mathbf{q}_2) = \frac{5}{7} + \frac{1}{2} \frac{\mathbf{q}_1 \cdot \mathbf{q}_2}{q_1 q_2} \left(\frac{q_1}{q_2} + \frac{q_2}{q_1} \right) + \frac{2}{7} \frac{(\mathbf{q}_1 \cdot \mathbf{q}_2)^2}{q_1^2 q_2^2}, \tag{2-9a}$$

$$G_2^{(s)}(\mathbf{q}_1, \mathbf{q}_2) = \frac{3}{7} + \frac{1}{2} \frac{\mathbf{q}_1 \cdot \mathbf{q}_2}{q_1 q_2} \left(\frac{q_1}{q_2} + \frac{q_2}{q_1} \right) + \frac{4}{7} \frac{(\mathbf{q}_1 \cdot \mathbf{q}_2)^2}{q_1^2 q_2^2}. \tag{2-9b}$$

The perturbation theory kernels have the following properties (Goroff et al. 1986, Wise 1988):

1. As $\mathbf{k} = \mathbf{q}_1 + \ldots + \mathbf{q}_n$ goes to zero, but the individual $\mathbf{q}_i$ do not, $F_n^{(s)} \propto k^2$. This is a consequence of momentum conservation in center of mass coordinates.

2. As some of the arguments of $F_n^{(s)}$ or $G_n^{(s)}$ get large but the total sum $\mathbf{k} = \mathbf{q}_1 + \ldots + \mathbf{q}_n$ stays fixed, the kernels vanish in inverse square law. That is, for $p \gg q_i$, we have:

$$F_n^{(s)}(\mathbf{q}_1, \ldots, \mathbf{q}_{n-2}, \mathbf{p}, -\mathbf{p}) \approx G_n^{(s)}(\mathbf{q}_1, \ldots, \mathbf{q}_{n-2}, \mathbf{p}, -\mathbf{p}) \propto k^2/p^2. \tag{2-10}$$

3. If one of the arguments $\mathbf{q}_i$ of $F_n^{(s)}$ or $G_n^{(s)}$ goes to zero, there is an infrared divergence of the form $\mathbf{q}_i/q_i^2$. This comes from the infrared behavior of the mode coupling functions $\alpha(\mathbf{k}, \mathbf{k}_1)$ and $\beta(\mathbf{k}, \mathbf{k}_1, \mathbf{k}_2)$. There are no infrared divergences as partial sums of several wavevectors go to zero.

2.3. Diagrammatic Expansion of Statistical Quantities

In this work we focus on the non-linear evolution of two-point cumulants of the density field, such as the power spectrum and the volume-average two-point correlation function, and their 1-point counterpart, the variance. These are defined respectively by:

$$\left\langle \tilde{\delta}(\mathbf{k}, \tau) \tilde{\delta}(\mathbf{k}', \tau) \right\rangle_c = \delta_D(\mathbf{k} + \mathbf{k}') P(k, \tau), \tag{2-11}$$

$$\bar{\xi}(R, \tau) \equiv \int \xi(x, \tau) \bar{W}(x) d^3x = \int P(k, \tau) W(kR) d^3k, \tag{2-12}$$

$$\sigma^2(R, \tau) = \int P(k, \tau)\ W^2(kR)\ d^3k. \tag{2-13}$$

Here $\xi(x, \tau) = \int P(k, \tau)\ \exp(i\mathbf{k} \cdot \mathbf{x})\ d^3k$ is the two-point correlation function, and $\bar{W}(x)$ is a window function, with Fourier transform $W(kR)$ which we take to be either a top-hat (TH) or a Gaussian (G),

$$W_{\rm TH}(u) = \frac{3}{u^3}\Big[\sin(u) - u\cos(u)\Big], \tag{2-14}$$

$$W_{\rm G}(u) = \exp(-u^2/2). \tag{2-15}$$

We are interested in calculating the non-linear evolution of these statistical quantities from Gaussian initial conditions in the weakly non-linear regime, $\sigma(R) \lesssim 1$. A systematic

framework for calculating correlations of cosmological fields in perturbation theory has been formulated using diagrammatic techniques (Goroff et al. 1986, Wise 1988, Scoccimarro & Frieman 1996). In this approach, contributions to p-point cumulants of the density field come from connected diagrams with p external (solid) lines and $r = p - 1, p, \ldots$ internal (dashed) lines. The perturbation expansion leads to a collection of diagrams at each order, the leading order being tree-diagrams, the next to leading order 1-loop diagrams and so on. In each diagram, external lines represent the spectral components of the fields we are interested in (e.g., $\delta(\mathbf{k}, \tau)$). Each internal line is labeled by a wave-vector that is integrated over, and represents a linear power spectrum $P_{11}(q, \tau)$. Vertices of order n (i.e., where n internal lines join) represent a $n^{\rm th}$ order perturbative solution δ_n, and momentum conservation is imposed at each vertex. Figure 1 shows the factors associated with vertices and internal lines. To find the contribution of order $2r$ to the *p-point spectrum* of the density field proceed as follows (Scoccimarro & Frieman 1996):

- Draw all distinct connected diagrams containing p vertices (with external lines labeled by $\mathbf{k}_1 \ldots \mathbf{k}_p$) joined by r internal lines. Two diagrams are distinct if they cannot be deformed into each other by moving the vertices and lines without cutting any internal lines (sliding lines over other lines is allowed in the rearrangement process). For each of these diagrams:

  1. Assign a factor of $\delta_D(\mathbf{k}_i - \mathbf{q}_1 - \ldots - \mathbf{q}_n) F_n^{(s)}(\mathbf{q}_1, \ldots, \mathbf{q}_n)$ to each vertex of order n and external momentum $\mathbf{k}_i$ $(i = 1, \ldots, p)$. For the arguments of $F_n^{(s)}$, we use the convention of assigning a positive sign to wave-vectors outgoing from the vertex.
  2. Assign a factor of $P_{11}(q_j, \tau)$ to each internal line labeled by $\mathbf{q}_j$.
  3. Integrate over all $\mathbf{q}_j$ $(j = 1, \ldots, r)$.
  4. Multiply by the symmetry factor of the graph, which is the number of permutations of linear fluctuations (δ_1's) that leaves the graph invariant.
  5. Sum over distinct labelings of external lines, thus generating $p!/(n_1! \ldots n_{2r-p+1}!)$ diagrams (where n_i denotes the number of vertices of order i).

- Add up the resulting expressions for all these diagrams.

To calculate 1-point cumulants, we have to integrate further over the $\mathbf{k}_i$ $(i = 1, \ldots p)$. These integrations are trivial because of the presence of delta functions given by rule 1, so we are left only with integrations over the $\mathbf{q}_j$'s. Also, since the $p!/(n_1! \ldots n_{2r-p+1}!)$ diagrams generated by rule 5 become equal contributions when the integration over external lines is performed, to find the contribution of order $2r$ to the *p^{th}-order 1-point cumulant* of the density field we replace rule 5 by the following:

- 5a. Integrate over $\mathbf{k}_i$ $(i = 1, \ldots p)$ and multiply by the multinomial weight $p!/(n_1! \ldots n_{2r-p+1}!)$.

Furthermore, when calculating cumulants of the *smoothed* density field, we add a window function at each vertex, giving instead of rule 1 (see Fig. 1):

- 1a. Assign a factor of $\delta_D(\mathbf{k}_i - \mathbf{q}_1 - \ldots - \mathbf{q}_n) F_n^{(s)}(\mathbf{q}_1, \ldots, \mathbf{q}_n) W(k_i R)$ to each vertex of order n and external momentum $\mathbf{k}_i$ $(i = 1, \ldots, p)$.

According to the above diagrammatic rules, we can write the loop expansion for the power spectrum up to one-loop corrections as

$$P(k,\tau) = P^{(0)}(k,\tau) + P^{(1)}(k,\tau) + \ldots, \tag{2-16}$$

where the superscript (n) denotes an n-loop contribution, the tree-level (0-loop) contribution is just the linear spectrum,

$$P^{(0)}(k,\tau) = P_{11}(k,\tau), \tag{2-17}$$

with $a^2(\tau)\langle \delta_1(\mathbf{k}) \delta_1(\mathbf{k}') \rangle_c = \delta_D(\mathbf{k} + \mathbf{k}') P_{11}(k,\tau)$, and the 1-loop contribution consists of two terms,

$$P^{(1)}(k,\tau) = P_{22}(k,\tau) + P_{13}(k,\tau), \tag{2-18}$$

with (see Fig. 2):

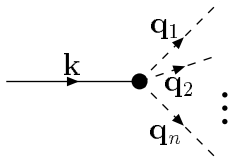

$$\equiv \quad \delta_D(\mathbf{k} - \mathbf{q}_1 - \ldots - \mathbf{q}_n) F_n^{(s)}(\mathbf{q}_1, \ldots, \mathbf{q}_n) W(kR)$$

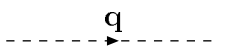

$$\equiv \quad P_{11}(q,\tau)$$

Fig. 1.— Diagrammatic rules for vertices and internal lines for density field fluctuations smoothed with window W at radius R.

$$P_{22}(k,\tau) \equiv 2\int [F_2^{(s)}(\mathbf{k}-\mathbf{q},\mathbf{q})]^2 P_{11}(|\mathbf{k}-\mathbf{q}|,\tau)P_{11}(q,\tau)d^3q, \quad (2\text{-}19a)$$

$$P_{13}(k,\tau) \equiv 6\int F_3^{(s)}(\mathbf{k},\mathbf{q},-\mathbf{q})P_{11}(k,\tau)P_{11}(q,\tau)d^3q. \quad (2\text{-}19b)$$

Here P_{ij} denotes the amplitude given by the above rules for a connected diagram representing the contribution from $\langle\delta_i\delta_j\rangle_c$ to the power spectrum. We have assumed Gaussian initial conditions, for which P_{ij} vanishes if $i+j$ is odd.

For the smoothed variance and average two-point correlation function we write

$$\sigma^2(R) = \sigma_\ell^2(R)\Big(1 + s^{(1)}\ \sigma_\ell^2(R) + \ldots\Big), \quad (2\text{-}20a)$$

$$\bar{\xi}(R) = \bar{\xi}_\ell(R)\Big(1 + x^{(1)}\ \bar{\xi}_\ell(R) + \ldots\Big), \quad (2\text{-}20b)$$

where $\sigma_\ell^2(R)$ and $\bar{\xi}_\ell(R)$ denote the variance and average two-point correlation function in linear theory (given by (2-13) and (2-12) with $P = P_{11}$); the dimensionless 1-loop amplitudes are

$$s^{(1)}(R) \equiv \frac{1}{\sigma_\ell^4(R)}\int P^{(1)}(k,\tau)\ W^2(kR)\ d^3k, \quad (2\text{-}21a)$$

$$x^{(1)}(R) \equiv \frac{1}{\bar{\xi}_\ell^2(R)}\int P^{(1)}(k,\tau)\ W(kR)\ d^3k. \quad (2\text{-}21b)$$

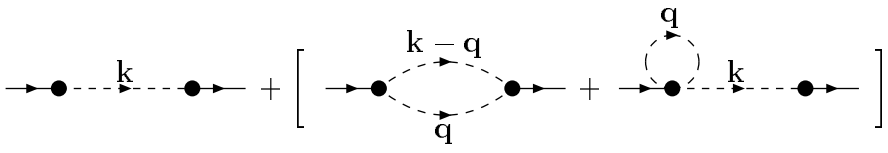

(P_{11}) (P_{22}) (P_{13})

Fig. 2.— Diagrams for the power spectrum up to one loop. See Eqs. (2-19) for diagram amplitudes.

A convenient property of these dimensionless amplitudes is the following: if one defines the correlation length $R_0^{(\ell)}$ in linear theory as the scale where the smoothed linear variance is unity, $\sigma_\ell^2(R_0^{(\ell)}) = 1$, then $s^{(1)}(R_0^{(\ell)}) = \sigma^2(R_0^{(\ell)}) - 1$ is just the non-linear correction to the variance at this scale.

3. Results

3.1. One-Loop Power Spectrum

We consider a linear (tree-level) power spectrum $P_{11}(k,\tau)$ given by a truncated power-law,

$$P_{11}(k,\tau) \equiv \begin{cases} A\ a^2(\tau)\ k^n & \text{if } \epsilon \le k \le k_c, \\ 0 & \text{otherwise,} \end{cases} \tag{3-1}$$

where A is a normalization constant, and the infrared and ultraviolet cutoffs ϵ and k_c are imposed in order to regularize the required radial integrations (Scoccimarro & Frieman 1996). In a cosmological N-body simulation, they would correspond roughly to the inverse comoving box size and lattice spacing (or interparticle separation) respectively. In the absence of the cutoffs, the spectrum (3-1) would be scale-free. We write the one-loop power spectrum contributions as

$$P_{ij}(k,\tau) \equiv \pi A^2 a^4(\tau)\ k_c^{2n+3}\ p_{ij}(n;x,\Lambda), \tag{3-2}$$

where the dimensionless 1-loop spectrum $p^{(1)} = p_{22} + p_{13}$, and we have introduced dimensionless wavenumber variables,

$$x \equiv k/k_c, \qquad \Lambda \equiv k_c/\epsilon. \tag{3-3}$$

From Eq. (2-19a) we obtain (defining $t \equiv q/k_c$):

$$p_{22}(n;x,\Lambda) \equiv \frac{x^4}{49} \int_{1/\Lambda}^{1} dt\ t^n \int_{\lambda_{min}(x,t)}^{\lambda_{max}(x,t,\Lambda)} d\lambda\ (x^2+t^2-2xt\lambda)^{n/2-2}\ (3t-7x\lambda-10t\lambda^2)^2, \tag{3-4}$$

when $x \le 2$; otherwise $p_{22}(n;x,\Lambda) = 0$. The constraint on the angular integration variable $\lambda \equiv (\mathbf{k}\cdot\mathbf{q})/(kq)$ comes from the cutoff dependence of $P_{11}(|\mathbf{k}-\mathbf{q}|,\tau)$, which gives:

$$\lambda_{min}(x,t) \equiv \mathrm{Max}\left\{-1, \frac{x^2+t^2-1}{2xt}\right\}, \tag{3-5a}$$

$$\lambda_{max}(x,t,\Lambda) \equiv \mathrm{Min}\left\{1, \frac{x^2+t^2-\Lambda^{-2}}{2xt}\right\}, \tag{3-5b}$$

Care must be taken when dealing with the limits imposed by Eqs. (3-5a) and (3-5b), especially in the cases $n = -1, -2$. On the other hand, integration over angular variables in Eq. (2-19b) is straightforward, and we obtain:

$$\begin{aligned} p_{13}(n;x,\Lambda) \;\equiv\; & x^n \int_{1/\Lambda}^{1} dt\; t^{n+2} \left[\frac{(6x^6 - 79x^4t^2 + 50x^2t^4 - 21t^6)}{63x^2t^4} + \frac{(t^2-x^2)^3\,(7t^2+2x^2)}{42x^3t^5} \right. \\ & \left. \times \ln\frac{|x+t|}{|x-t|} \right], \end{aligned} \tag{3-6}$$

for $\Lambda^{-1} \le x \le 1$; otherwise $p_{13}(n;x,\Lambda) = 0$.

In the following subsections we give results for p_{13} and p_{22} in the limit $\Lambda = k_c/\epsilon \to \infty$ up to terms of order Λ^0, for spectral indices $n = 1, 0, -1, -2$. We also give their asymptotic behavior at large scales. From the properties of the perturbation theory kernels given in Sec. 2.2 and Eqs. (2-19), one would naively expect that as $x \to 0$:

$$p_{22}(n;x,\Lambda) \propto x^4 \sim (k/k_c)^4, \qquad p_{13}(n;x,\Lambda) \propto x^{n+2} \sim (k/k_c)^{n+2}. \tag{3-7}$$

Although this is certainly correct for p_{22} when $x \ll \Lambda^{-1}$ (i.e., $k \ll \epsilon$), the expressions below correspond to p_{22} and p_{13} *after* the limit $\Lambda \to \infty$ has been taken and therefore exhibit a different kind of asymptotic behavior (corresponding to $0 \leftarrow \epsilon < k \ll k_c$). This deviation from the expected scaling becomes more pronounced as n decreases, since infrared effects ($\epsilon \to 0$) become more important with the increase of large-scale power. As we will see, Eq. (3-7) is obeyed by p_{22} only when $n \ge 1$ and by p_{13} when $n \ge 0$.

Our results below are equivalent to those of Makino et al. (1992) in the case of p_{13}, but they differ for p_{22} in two respects. First, their expressions for p_{22} are only valid for $x < 1$; they did not seem to consider that p_{22} is non-vanishing up to $x = 2$, and the region $1 \le x \le 2$ requires a separate integration when n is odd. In addition, for n even, their series expansions for the dilogarithms do not converge in this region. The second difference comes from the fact that for $n = -1, -2$, p_{22} develops a divergence at $x = 1$, and the expressions

for p_{22} must be modified in a region of radius Λ^{-1} about $x = 1$. This singularity is integrable, giving a finite contribution to the 1-loop correction to the variance. Finally, some of their resulting expressions for $p^{(1)}$ contain typographic errors. We have checked our expressions by analytically integrating them and verifying that they correctly reproduce the unsmoothed 1-loop coefficients $s^{(1)}$ given by Scoccimarro & Frieman (1996). For comparison, we also plot (but do not give explicit expressions for) the 1-loop power spectrum in the Zel'dovich approximation.

3.1.1. $n = 1$

For $n = 1$, the dimensionless 1-loop power spectrum contributions are

$$p_{13}(1;x) = -\frac{1}{21x} + \frac{52x}{315} - \frac{181x^3}{315} - \frac{2x^5}{21} + \ln\left(\frac{1+x}{1-x}\right)\frac{(5 - 19x^2 + 25x^4 - 5x^6 + 10x^8)}{210x^2} + \frac{8x^5}{105}\ln\left(\frac{1-x^2}{x^2}\right), \tag{3-8}$$

$$p_{22}(1;x) = \frac{18x^4}{49} - \frac{13x^5}{98} - \frac{20x^6}{1029} + \frac{x^7}{49}, \qquad \text{if } x \le 1, \tag{3-9}$$

$$p_{22}(1;x) = -\frac{320}{1029x} + \frac{16x}{49} + \frac{2x^3}{3} - \frac{18x^4}{49} - \frac{5x^5}{42} + \frac{20x^6}{1029} + \frac{x^7}{49}, \qquad \text{if } 1 \le x \le 2, \tag{3-10}$$

and the 1-loop reduced power spectrum is then (see Fig. 3):

$$p^{(1)}(n=1; x = k/k_c \le 1) = -\frac{1}{21x} + \frac{52x}{315} - \frac{181x^3}{315} + \frac{18x^4}{49} - \frac{67x^5}{294} - \frac{20x^6}{1029} + \frac{x^7}{49} + \ln\left(\frac{1+x}{1-x}\right)\frac{(5 - 19x^2 + 25x^4 - 5x^6 + 10x^8)}{210x^2} + \frac{8x^5}{105}\ln\left(\frac{1-x^2}{x^2}\right), \tag{3-11}$$

with $p^{(1)}(x) = p_{22}(x)$ when $1 \le x \le 2$. For $x \ll 1$ we get:

$$p_{13}(1;x) \approx p^{(1)}(1;x) \approx -\frac{122}{315}x^3 + \mathcal{O}(x^5), \tag{3-12}$$

$$p_{22}(1;x) \approx \frac{18}{49}x^4 + \mathcal{O}(x^5). \tag{3-13}$$